GPS/Loran–C Interoperability for Time and Frequency Applications—A Survey of the Times of Arrival of Loran–C Transmissions via GPS Common Mode/Common View Satellite Observations

Bruce Penrod, Richard Funderburk, Peter Dana–Consultant
Austron, Inc.
P.O. Box 14766
Austin, Texas 78761

I. Introduction

Since the advent of GPS satellite based time and frequency transfer the role of Loran–C in this application has been greatly diminished. The capabilities of undegraded GPS are indeed superior to those of the Loran–C system in most respects including coverage, absolute timing accuracy, and ease of use. However potential drawbacks of GPS to the time and frequency user exist, such as higher cost, more complex hardware and non–civilian control of the system. This last has brought us the specter of Selective Availability (SA), an on again–off again, intentional degradation of the accuracies obtainable from the GPS. Though not the focus of this report, it should be noted that the medium term (τ =780 seconds) frequency stability of the Loran–C transmissions, for reasonably close transmitters, is almost two orders of magnitude better than that of the GPS transmissions observed under SA—reason enough to keep Loran–C in mind for frequency control purposes.

This paper surveys the absolute time setting performance achievable from seven distinct transmitters in four North American chains via the Loran–C Time of Coincidence (TOC) with UTC synchronization technique. Motivation for this undertaking consisted of both frustration with SA and strong curiousity about how well the propagation path of the Loran–C signals could be modeled and how well the transmitters are synchronized to UTC as a result of the enactment in 1987 of Public Law 100–223[2] requiring synchronization at the 100 ns level. Navigation users desiring to combine GPS with Loran–C to enhance the overall reliability of their systems would prefer to treat the Loran–C signals analogously to those from the satellites, i.e. as pseudo–ranges rather than as time differences (TD's), the input to the traditional Loran–C hyperbolic navigation solution. Multi–chain Loran–C navigation is also facilitated by absolute time synchronization as well.

The propagation modeling techniques applied in this study were intentionally limited to those which could be implemented in a modern, low cost microprocessor based instrument and therefore do not include the terrain inclusive, full wave integral approach. The results presented here support development of a new Loran–C timing receiver with internal propagation path correction and multiple chain capability offering precise time setting at the 500 ns level. While this performance is just comparable

to that of GPS under SA for absolute timing, the frequency stability is far superior and the equipment cost is much less.

II. Approach

The equipment for the experiment consists of an Austron Model 2201 GPS Timing and Frequency receiver, an Austron Model 2100T Loran–C Timing receiver, an HP–85 desktop computer for controlling the 2100T receiver, an antenna ambient temperature recorder and various PC's for processing and presenting the data. The 2201 GPS receiver is operated in the NIST/USNO time transfer mode where both the tracking of satellites and the processing of the acquired data are to the NIST/USNO specified format. Adherence to these specific requirements allows a differential time transfer mode of operation with various time standards laboratories worldwide who maintain receivers which track to the same specifications and make that data available to the public. The benefit of this common mode/common view operation is of course the complete removal of the satellite clock error and partial removal of orbital and ionospheric errors. Significant reduction of SA induced errors is also realized since they are a combination of satellite clock and ephemeris dithering.

Knowledge of the receiver positions at both ends of the link is of course required for this to work. Austron's position was transferred, via a differential GPS carrier phase survey, from the position of the Applied Research Laboratories of the University of Texas at Austin which is known to the one meter level in WGS 84. The time transfer accuracies attainable under these conditions are at the 10 ns level under the non–SA conditions experienced during the duration of the data taking.

The 2100T Loran–C receiver is operated in a sequence mode of operation under the control of the HP–85 desktop computer via the IEEE–488 bus. The HP–85 takes care of the parameter set–up for each of the ten Loran–C transmissions tracked over the data acquisition period. These include setting the Group Repetition Interval (GRI), secondary coding delays, and TOC synchronization times. All error messages generated by the 2100T such as blink, cycle error and loss of signal are logged by the HP–85 as well in order to facilitate outlier removal.

Data was acquired in both three hour and twenty–four hour dwell modes, according to this pattern: one ten day, three hour dwell period followed by one twenty day, twenty–four hour dwell period and finally one ten day, three hour dwell period. Additional data was then taken for about six days on the two weakest stations, Carolina Beach and Searchlight, to make up for significant gaps due to skywave tracking problems during the sequencing periods, and also on Dana to resolve GRI related anomalies in the TOA's which were noted during the sequencing periods.

After acquiring the Loran–C pulse and selecting the third cycle, the 2100T waits for the next TOC to synchronize its 1 PPS output to the arrival time of the UTC synchronized Loran–C pulse. If the Loran–C pulse does indeed arrive at the scheduled time then the receiver indicates that a successful TOC synchronization has occurred and sets its 1 PPS output to that time of arrival. This 1 PPS output is input to the 2201 GPS receiver which measures its relation in time to the received satellite currently being tracked and logs the data in the NIST/USNO format. Approximately twenty–four hours later the corresponding USNO track data is available for downloading over a modem and used to correct the previously acquired raw satellite data. These differential TOA's, now referenced to the USNO master clock, are then corrected for propagation path delays and analyzed with the temperature data.

III. Loran–C TOA Predictions

A. Background

All positions and path corrections are in the WGS–84 geodetic datum[1]. The Austron antenna position for both GPS and Loran–C is:

Receiver	Latitude	Longitude
Austron Site	+30:27:15.47	- 97:39:45.72

The Loran–C transmitters and their positions[2] are shown in Table 1.

TABLE 1. Loran–C Transmitter Locations

Transmitter	Latitude	Longitude
Malone	+30:59:38.870	– 85:10:08.751
Grangeville	+30:43:33.149	– 90:49:43.046
Raymondville	+26:31:55.141	– 97:49:59.539
Jupiter	+27:01:58.528	– 80:06:52.875
Carolina Beach	+34:03:46.208	– 77:54:46.100
Dana	+39:51:07.658	– 87:29:11.586
Searchlight	+35:19:18.305	–114:48:16.881

The conductivity data used for these predictions is a set of disk files: the FCC data base for microcomputers[3]. The FCC M3 map file data shown in Figure 1 is based on a study of effective ground conductivity for the United States[4]. The data, in the form of line segments that define conductivity boundaries, was accessed by a program written for this project that returns the conductivity for any latitude and longitude.

An ellipsoidal ray path is computed[5] from the Austron site to the Loran–C transmitter and with an arbitrary step size a set of latitudes and longitudes is created for looking up conductivities. The prediction program produces a list of ranges and conductivities along the path from receiver to transmitter.

The phase delay of a ground wave can be separated into two components: the primary phase and the secondary phase. The primary phase is the result of propagation through the air while the secondary phase is the result of propagation over a conducting surface with terrain variations. National Bureau of Standards Circular 573[7] defines the primary and secondary phase for the low frequency groundwave over homogeneous paths. The primary ground wave phase can be described as:

$$pf = \frac{dn}{c_0} \tag{1}$$

where:

$$pf = \text{primary phase (seconds)} \tag{2}$$

$$
\begin{aligned}
d &= \text{range meters} \\
c_0 &= \text{speed of light in vacuo (meters/sec)} \\
n &= \text{index of refraction of air}
\end{aligned}
$$

The index of refraction of air is influenced by pressure, temperature, and humidity[9]:

$$n = 1 + 0000776(P/T + 4810e/T^2) \tag{3}$$

where:

$$
\begin{aligned}
T &= \text{temperature (°K)} \\
P &= \text{atmospheric pressure (millibars)} \\
e &= \text{partial water vapor pressure}
\end{aligned} \tag{4}
$$

For most ground wave predictions, Loran–C in particular, a value for n is assumed to be 1.000338[7]. The value can change from 1.0002 to 1.0004[10]. The wave velocity at 100 kHz at the surface for a perfectly conducting ground and $n = 1.000338$ is then:

$$c = \frac{c_0}{n} = 299691162\ meters/second. \tag{5}$$

The secondary phase correction may be computed using the methods provided by NBS 573. The methods involve time consuming solutions of Legendre polynomials and Hankel functions. Faster methods have been developed for receiver implementation.

B. Brunavs' Polynomials

A faster method of obtaining secondary phase corrections from distance and conductivity in a real time receiver uses Brunavs' formulas[8]. The corrections applied here employ the eight coefficient implementation offering residual fit errors at the six meter level. The correction returned by the Brunavs formula, Eq. 6 is added to the primary phase correction to give the total path delay.

$$p = c_1 + c_2 s + (c_3 s + c_4)e^{c_5 s} + \frac{c_6}{1 + c_7 s + c_8 s^4} + \frac{2.277}{s}, \tag{6}$$

where:

$$
\begin{aligned}
s &= \text{range (meters)/100000} \\
p &= \text{phase lag (meters)} \\
c_i &= \text{eight coefficients for each conductivity}
\end{aligned} \tag{7}
$$

Application of Brunavs' formula to the mixed conductivity paths typically encountered is performed using three approaches: average conductivity, average complex impedance, and the Millington–Pressy[9]

technique. The first two techniques are essentially range segment length weighted averages of either the conductivity (real) or the impedance (complex) along the receiver to transmitter path. The impedance method requires the additional step of converting back to conductivity after the path integration[11]. The third approach is a heuristic method which has historically given good results near distinct impedance boundaries (coastlines), where it reproduces the localized phase disturbances near those boundaries. Table 2 presents the path data for each transmitter.

TABLE 2. Propagation Path Characteristics

Transmitter	Range (km)	Pri. Phase (μs)	Sec. Phase (μs)		
			Cond.	Imp	Mil–Pres.
Malone	1197.479	3995.710	6.881	6.550	5.847
Grangeville	656.048	2189.082	3.119	3.076	2.924
Raymondville	435.021	1451.563	1.618	1.598	1.560
Jupiter	1753.507	5851.047	6.546	5.490	5.970
Carolina Bch	1900.259	6340.725	9.953	9.741	9.569
Dana	1393.296	4649.107	6.188	6.102	5.910
Searchlight	1689.677	5638.062	7.520	7.464	7.052

C. Propagation Model Evaluation

1. Correction of Chain Timing Errors

As previously alluded, TOA data on some of the dual rated Loran–C transmitters exhibited anomalous behavior, i.e. a 5 μs difference between the same transmitter on a different chain GRI. Since there could be no path differences in these transmissions and since the receiver will only track positive zero crossings of the 100 kHz carrier, a flag was raised concerning phasing of the chain. This characteristic was observed on transmissions from Dana on GRI's 89700 and 99600 and from Carolina Beach on GRI's 79800 and 99600. In each case, the transmissions from the 99600 GRI were 5 μs later than the other GRI. The transmissions from Malone on GRI's 79800 and 89700 did not exhibit such a large difference, however. They differed by less than a microsecond. The transmissions from Searchlight on GRI 99400 fall in line with those from the North East chain on GRI 99600.

Conversations with the Loran–C timing personnel at the USNO and measurements made by them on November 28–29, 1990 confirmed these anomalies on Dana, Seneca and Carolina Beach[13]. The USNO measurements, made with an Austron Model 2100T receiver, place the transmissions on GRI 99600 on–time relative to the USNO Master Clock. Those from the 89700 and 79800 GRI's are 5 μs early. Based on this information, all data from these early arriving GRI's was corrected prior to further processing by the addition of exactly 5 μs to their TOA's.

2. Model Evaluation

Performance of each of the techniques on actual Loran–C TOA data taken from the Austron site is shown in Figures 2 and 3, which present data from two consecutive ten day twenty–four hour dwells on seven Loran–C transmitters, three of which are dual rated and seen twice each ten days. Each data trace has been corrected for propagation delay using one of the three methods described previously.

Regression analysis on the entire forty–seven days of data, corrected by each of the three methods, is summarized in Figure 4. The complex impedance approach yields the tightest cluster of TOA's with a residual RMS scatter of 463 ns. It also yields a TOA midway between those of the other two models. Since the Austron location is not near any significant impedance boundary, any advantages yielded by the Millington–Pressy approach may not be visible. In fact the method performs the most poorly of the three with a residual RMS scatter of 732 ns. The average conductivity approach is slightly better at 669 ns. The remainder of the data and analysis makes use only of the average complex impedance path correction.

IV. Results

A. Overall Performance

More than one thousand TOA's were logged over forty–seven days of testing. The vast majority of these NIST/USNO formatted points were complete 780 second tracks. For each of these time–tagged points an antenna temperature reading was collected. Figure 5 shows all of the data collected over the experiment, including the temperature trace. Linear regression analysis on this propagation corrected data versus time and temperature yields a frequency offset of 10.8 ns/day with +/-1.4 ns/day one sigma points, a temperature coefficient of -1.1 ns/deg C with +/-2.2 ns/deg C one sigma points (no significant temperature coefficient in this mixed data), and a residual standard deviation of 463 ns. From the regression data, the predicted GPS and Loran–C antenna, cable and receiver delays would be 53.418 μs at the time of the first data point on MJD 48169 (October 5, 1990).

The actual delays measured on the two receivers were:

Model 2201 GPS receiver	.047 μs	
Model 2100T Loran–C receiver	51.760 μs	(includes third cycle tracking delay)

The difference of these delays, 51.713 μs, should be the expected offset of the received Loran–C TOA's, as measured by the GPS receiver, from USNO via the common mode/common view technique. This implies that the realized absolute time transfer accuracy over the period of this test, including transmitters nearly two thousand kilometers away, is:

$$53.418\mu\text{s} - 51.713\mu\text{s} = 1.705\mu\text{s} \pm 1\sigma = .463\mu\text{s}$$

B. Individual Transmitter Performances

Figures 6 and 7 show two consecutive ten day periods of propagation delay corrected, twenty–four hour dwell TOA data with the antenna temperature shown on the bottom trace. Inspection of these charts shows that there are varying levels of temperature correlation in the received signals from the different transmitters as well as definite biases in the TOA's. Linear regression analyses on both time and temperature for each transmitter's set of data yield the results graphed in Figures 8 through 12.

Figure 8 shows the regressed TOA's at test startup, MJD 48169 (October 5, 1990) and the residual standard deviations for each transmitter. These TOA's vary from 52.8 μs to 53.9 μs across the transmitters while the residual standard deviations vary from less than 100 ns to over 500 ns.

Figures 9 and 10 show the regression coefficients (slopes) for time and temperature along with their standard deviations. The temporal slope varies from 2 ns/day to 18 ns/day (low parts in 10^{13} fractional frequency offset), and the temperature coefficients range from -2 ns/deg C to almost 45 ns/deg C. This latter level, from the Searchlight transmitter, is almost certainly not actually temperature induced but is more likely skywave induced. The levels of the other six transmitters, ranging from -2 ns/deg C to 8 ns/deg C are in reasonable agreement with those reported in previous proceedings of this conference[12].

Since the data taken for this survey covers transmitters located from 400 km to nearly 2000 km from the Austron site, some correlation should be observable between both the residual standard deviations of the TOA's and the temperature coefficients. Figure 11 plots the regression residual standard deviation against the range in kilometers divided by the square root of the peak radiated power in watts (very much a first order approximation to received signal to noise ratio). Though not perfectly correlated, especially in the more distant transmitters, a definite relationship is evident. Figure 12 plots the regression temperature coefficient versus range. Here as well a strong overall trend is evident. The Jupiter transmitter with its very small and negative coefficient, whose path contains the only sea water of the transmitters tracked, falls completely out of line with the other transmitters. The Dana transmitter also displays unexpectedly good temperature insensitivity considering the length of the path.

V. Conclusions

The results from this survey (even ignoring the systematic 5 μs error) clearly indicate that the GPS time transfer capability is superior to that of the Loran–C system for absolute timing accuracy, and that even with the most careful calibration of the Loran–C receiver delay and propagation path, inexplicable TOA biases remain which are larger than the variations across all of the transmitters. Much more data covering years would be needed to show that these biases were stable enough to be removed with a one time site calibration.

The syntonization of the transmissions is excellent, all showing low parts in 10^{13} offsets versus the USNO master clock. With the exception of the Searchlight transmitter, all of the transmissions exhibit timing stabilities over the entire period of less than 300 ns RMS which is at the observed levels of GPS under SA. As previously mentioned though, the Loran–C phase instabilities take place over a much greater time interval than those being forced onto the GPS signals under SA, providing far better medium to short term frequency stability. This is shown in Figure 13 where 780 second observations of the Loran–C received fractional frequency offsets have been combined in a RMS sense and plotted versus transmitter and range/square root power ratio. From this data it can be seen that all but the most distant transmitters offer better than three parts in 10^{11} stability at this averaging time. It is in the frequency control area where GPS/Loran–C interoperation will offer some synergistic advantages over GPS alone under SA.

Synchronization of the chains to UTC as required by Public Law 100–223 has obviously not been accomplished at this time.

VI. References

1. Department of the Air Force, WGS 84 Defining Parameters and Derived Constants, HQ USAF Space Division, Los Angeles, 1987.

2. U.S. Coast Guard, Radionavigation Bulletin, Number 23, U.S. Department of Transportation, Washington, DC, 1990.

3. FCC, FCC M3 Map Data File for Microprocessors, NTIS PB87- 222253, Washington, DC, 1981.

4. Fine, H., *An Effective Ground Conductivity Map for Continental United States,* Proceedings of the IRE, September, 1954.

5. Snyder, J. P., Map Projections Used by the U.S. Geological Survey, USGS 1532, Washington, DC, 1982.

6. U.S. Coast Guard, Specification of the Transmitted Loran-C Signal, USCG COMDTINST MI6562.4, U.S. Department of Transportation, Washington, DC, July, 1981.

7. Johler, J. R., et al, Phase of the Low Frequency Ground Wave, NBS Circular 573, Washington, DC, 1956.

8. Brunavs, P., Phase Lags of 100kHz Radiofrequency Groundwave and Approximate Formulas for Computation, Canadian Hydrographic Service Internal Report, 1977.

9. Samaddar, S. N., *The Theory of Loran-C Ground Wave Propagation—A Review,* Journal of the Institute of Navigation, Vol. 26, No. 3, Washington, DC, 1979.

10. Doherty, R. H., L. W. Campbell, S. N. Samaddar and J. R. Johler, *A Meteorological Prediction Technique for Loran-C Temporal Variations,* Wild Goose Association, Williamsburg, VA, 1979.

11. Johler, J. R., Loran-C Pulse Transient Propagation, U.S. Dept. of Transportation, NTIS AD A077551, Washington, DC, 1979.

12. Markovic, Zoran M., *Meteorological Influences on Loran-C Propagation Over Sea and Land in Mediterranean Sea Chain,* Proceedings of the Twentieth Annual Precise Time and Time Interval (PTTI) Applications and Planning Meeting, Washington, DC, 1988.

13. Telecons with Mihran Miranian of the USNO, November 21–30, 1990.

FIG. 1--ECC M3 Conductivity Map

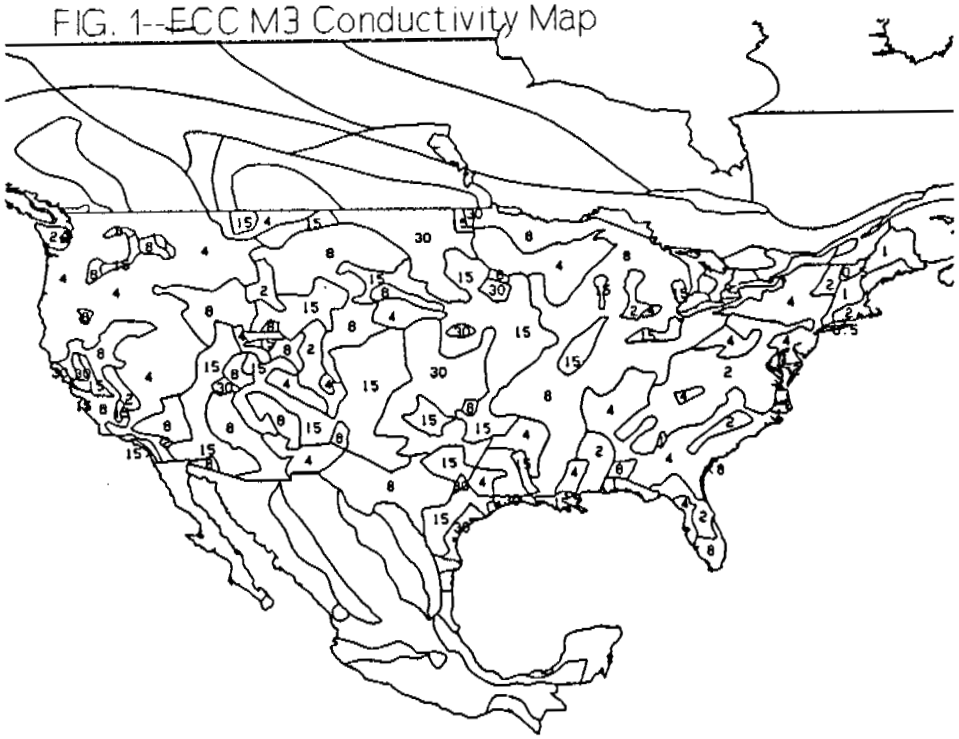

FIG. 2--Loran-C TOA's, 24 Hour Dwells, Various Propagation Models

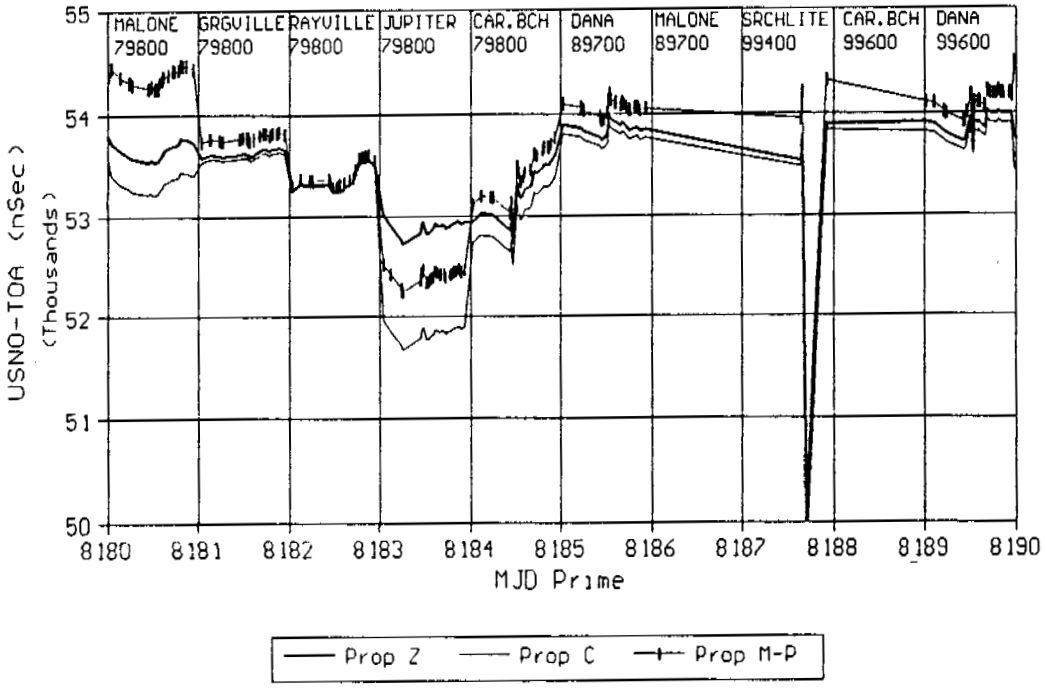

FIG. 3--Loran-C TOA's, 24 Hour Dwells, Various Propagation Models

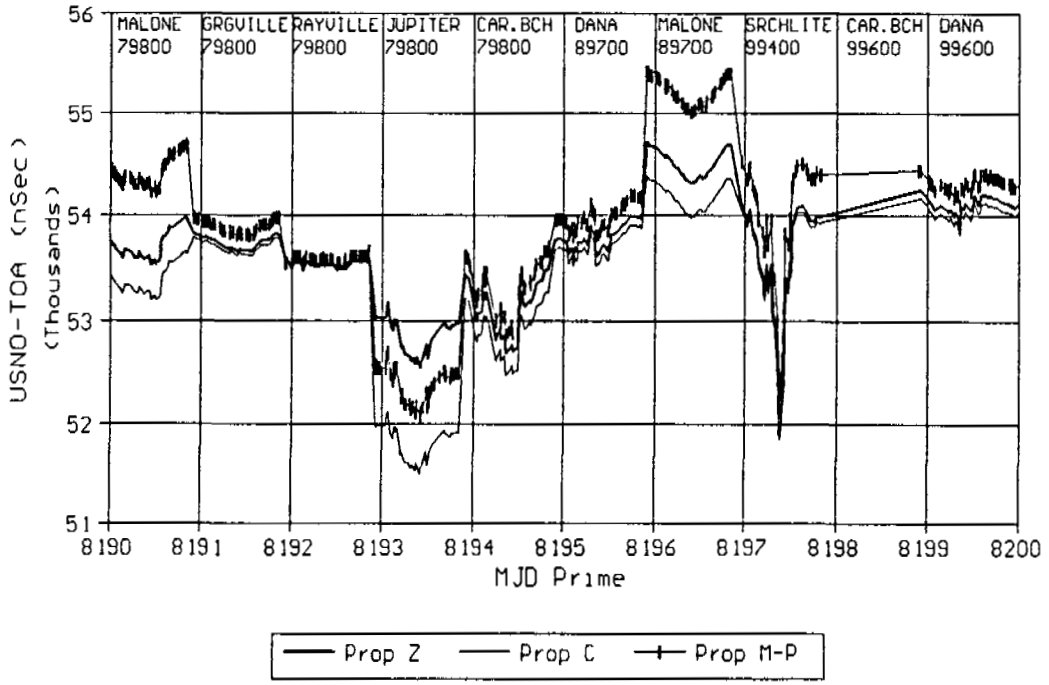

FIG. 4--Loran-C TOA's, Residual RMS, from Time/Temp Regression

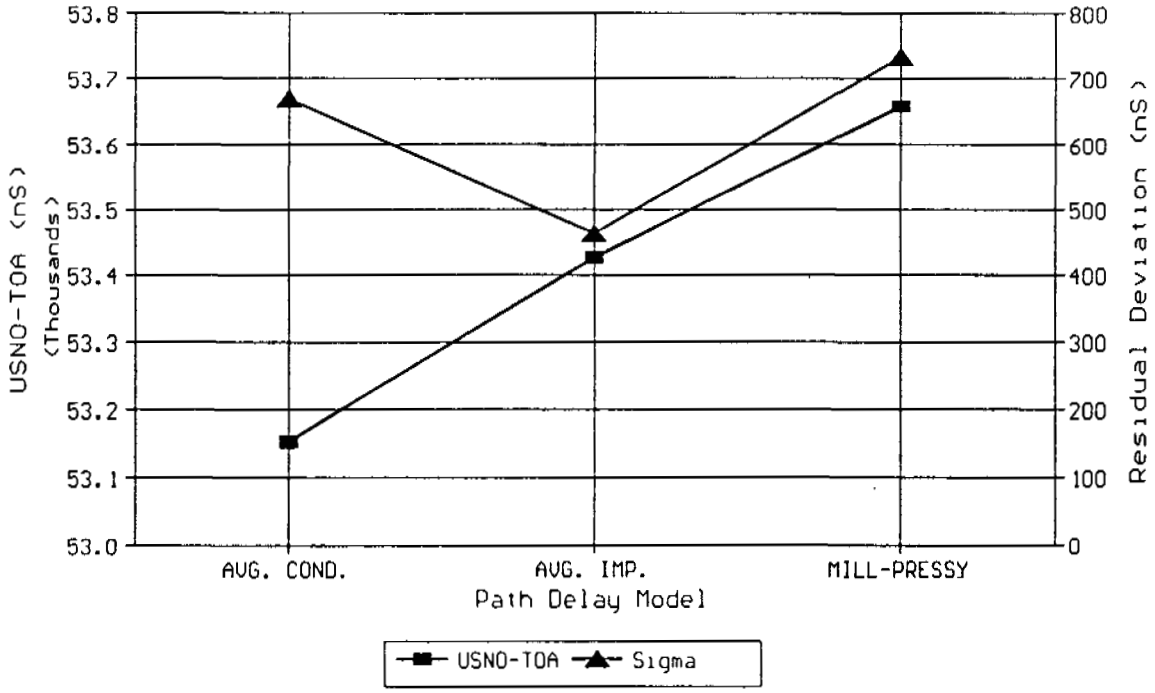

FIG. 5--Loran-C TOA's, 3 Hour/24 Hour Dwells vs Antenna Temperature

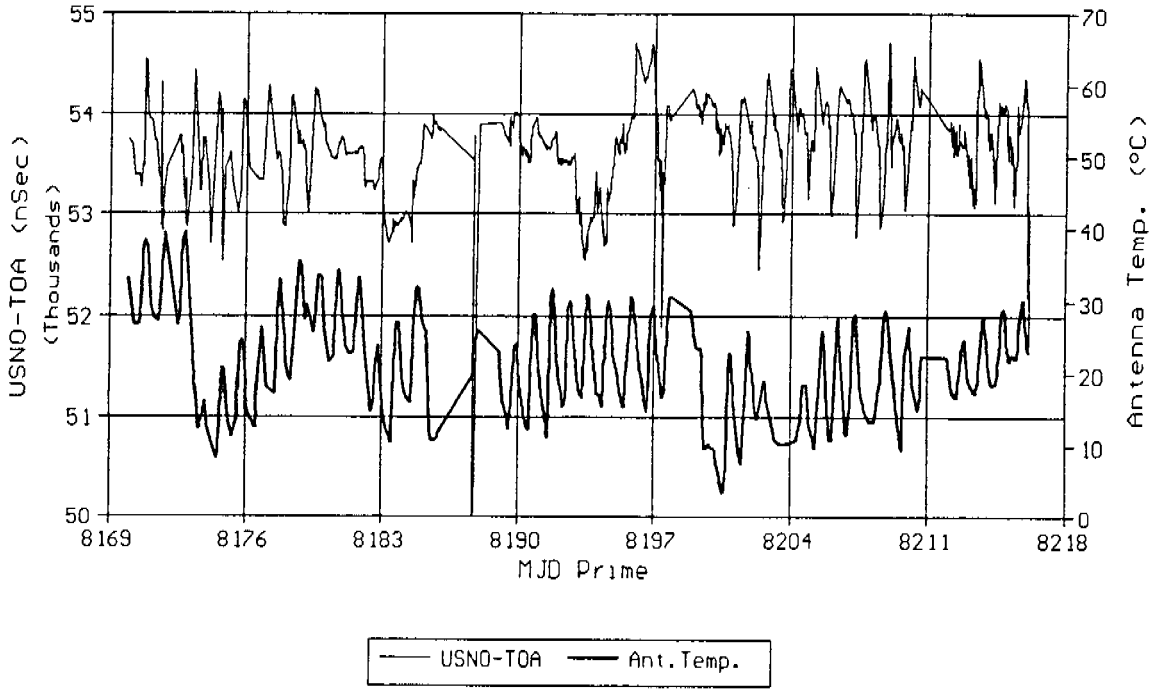

FIG. 6--Loran-C TOA's, 24 Hour Dwells vs Antenna Temperature

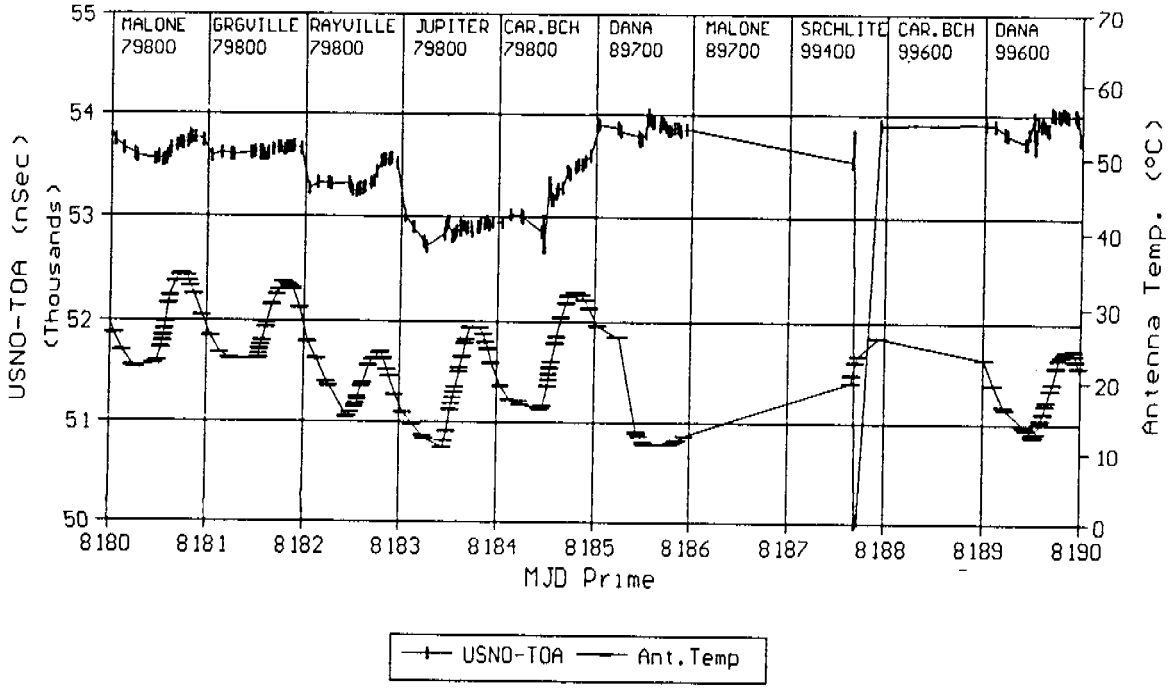

FIG. 7--Loran-C TOA's, 24 Hour Dwells
vs Antenna Temperature

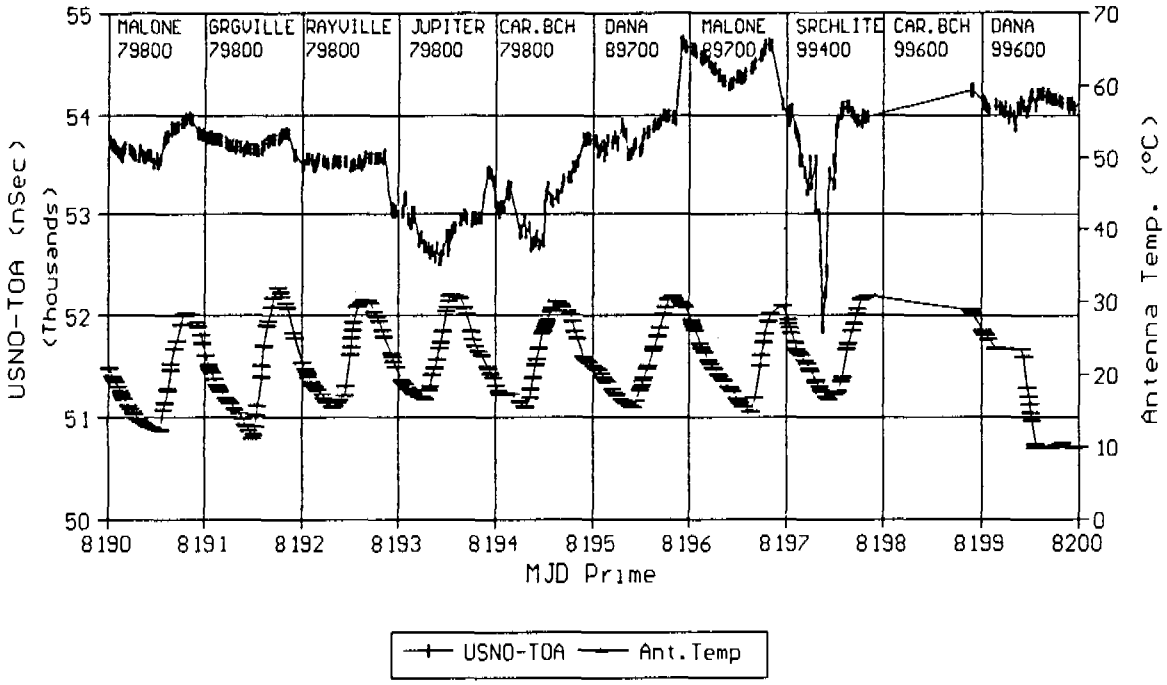

FIG. 8--Loran-C TOA's and Residual RMS
from Time/Temp Regression

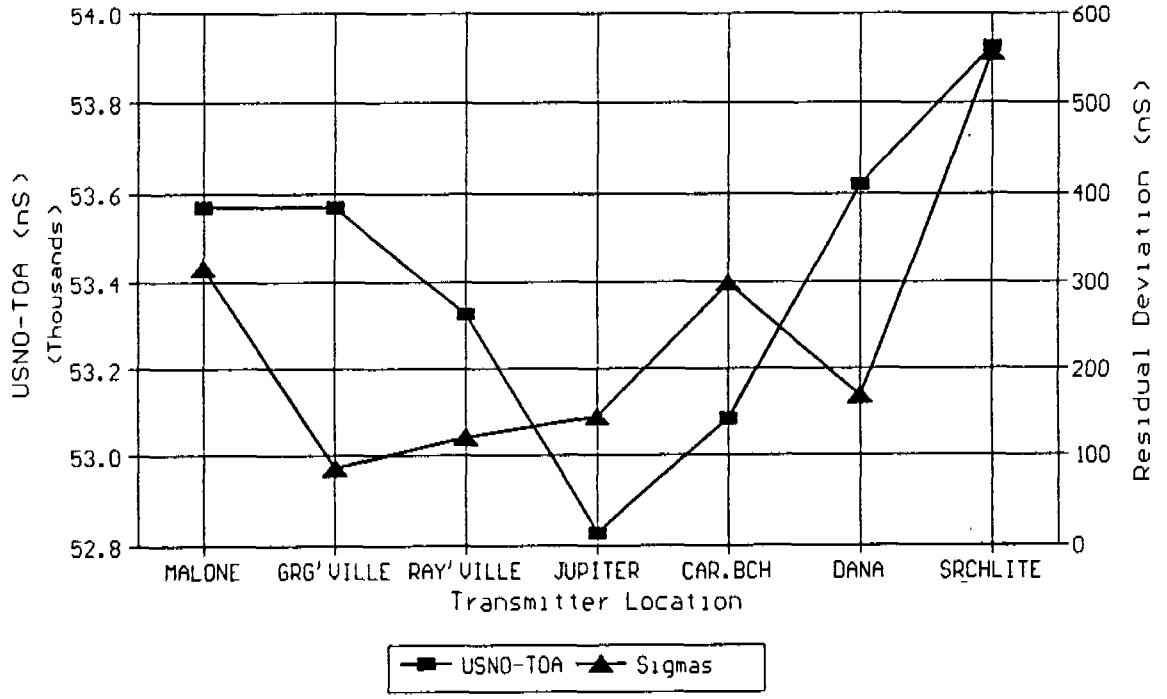

FIG. 9--Loran-C δ(USNO-TOA)/δt and Sigma from Time/Temp Regression

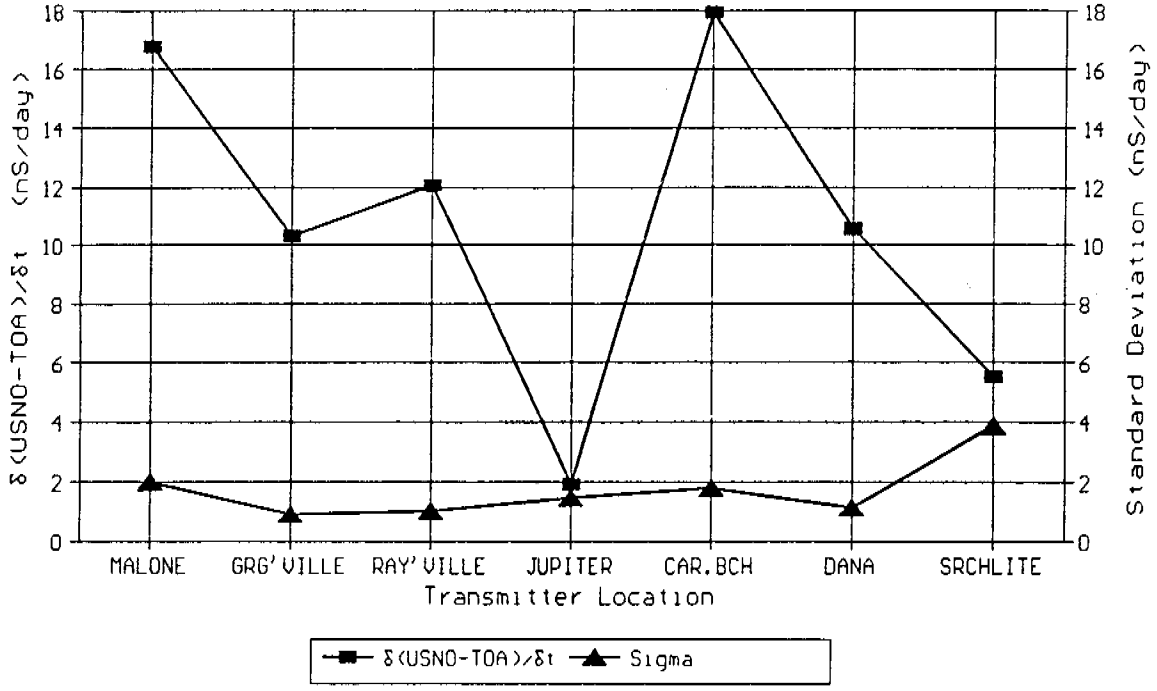

FIG. 10--Loran-C δ(USNO-TOA)/δT and Sigma from Time/Temp Regression

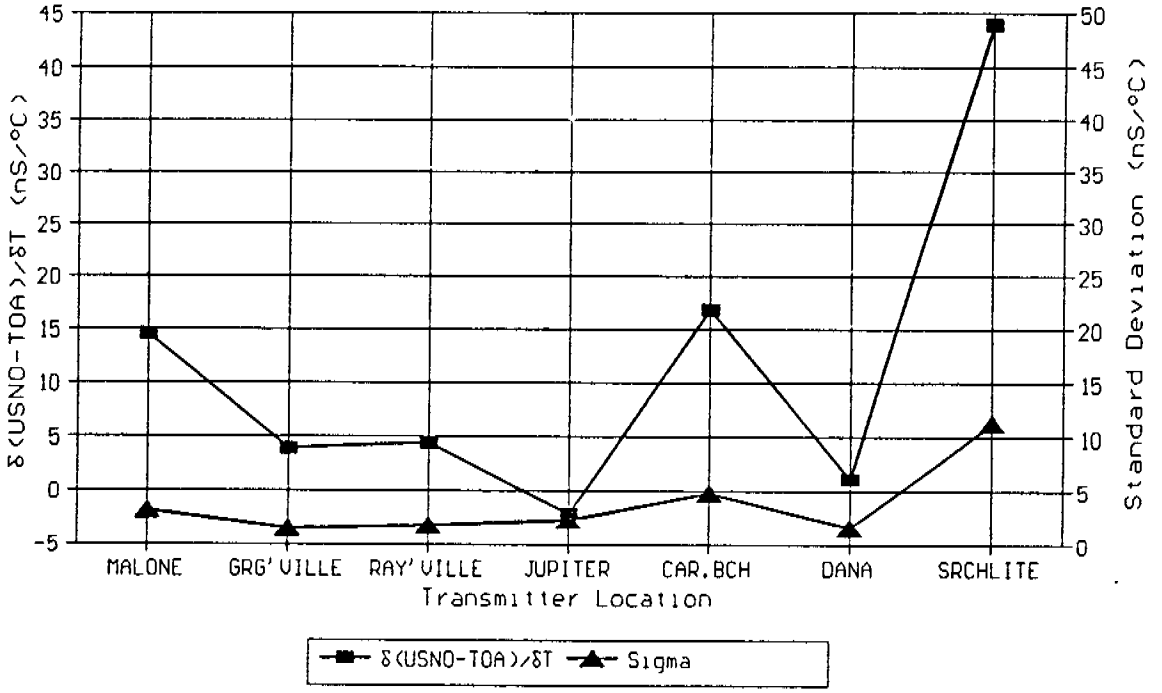

FIG. 11--Loran-C Residual RMS vs. R/√P
from Time/Temp. Regression

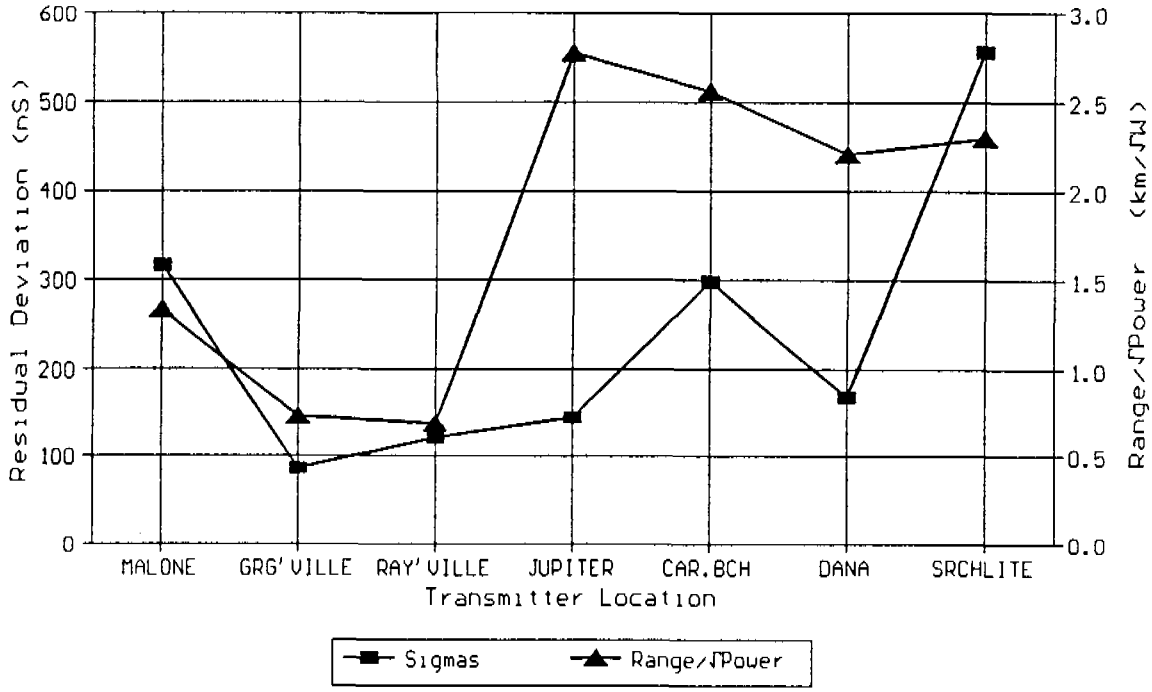

FIG. 12--Loran-C δ(USNO-TOA)/δT vs Range
from Time/Temp. Regression

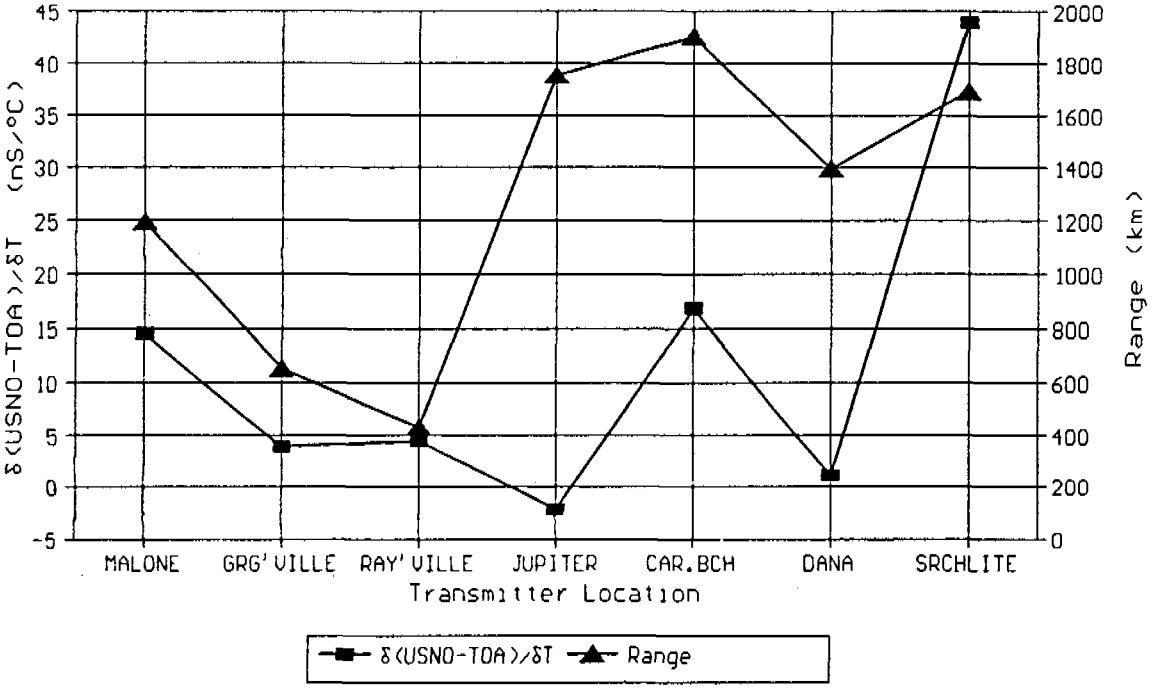

FIG. 13--Loran-C RMS δf/f @ γ=780 sec
from GPS Time Transfer Data

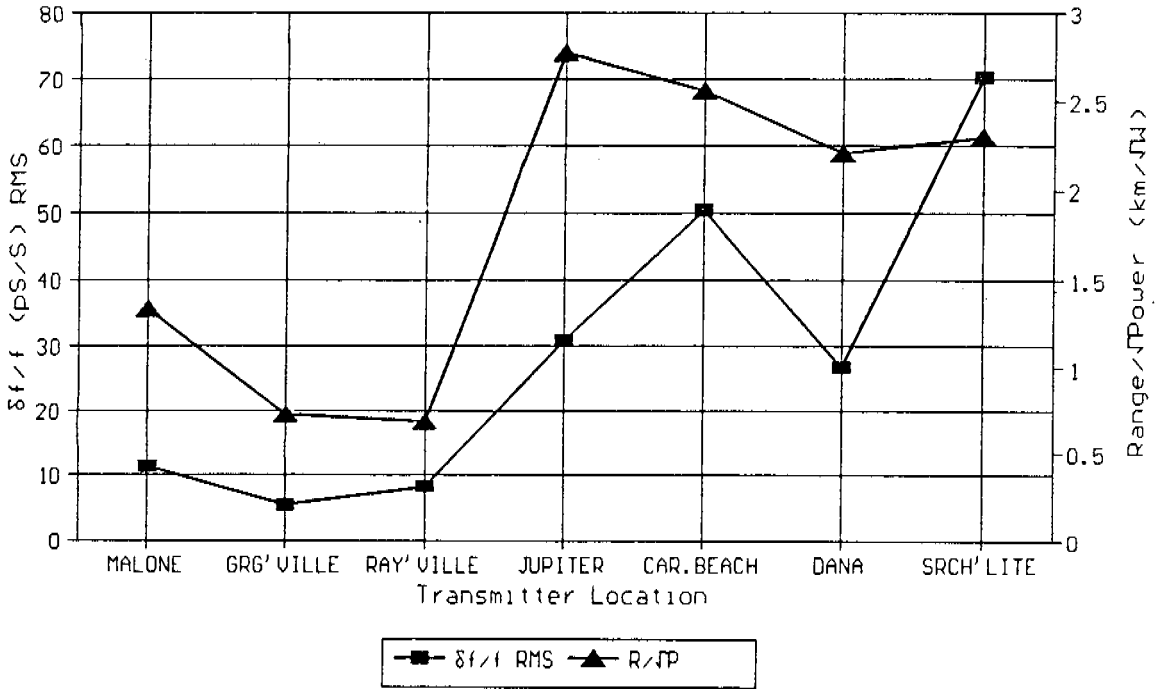

QUESTIONS AND ANSWERS

Dr Winkler, U. S. Naval Observatory: I would like to make some comments regarding your interesting presentation. Number one, your conclusions are completely consistent with my own. I think that you have done an excellent job. Number two, I would suggest that, in addition to the disturbances and causes for noise which you have mentioned, there is one which is particularly important in the Washington metropolitan area. That is interference. Interference, as it comes on and goes off, will, depending on the position of the filters in the preamplifiers, affect the bias in the receivers. This is quite a problem and it is part of our efforts to improve our capabilities in our monitoring. That leads me to the third point and that is your conclusion that the Public Law requirement has not been realized. I would say 'not yet been realized' because there are considerable efforts going on which have been hampered by the lack of funding. Congress passed a law without regular and well organized funding procedure. Under the funding limitations which now exist, the problems of truly synchronizing all of the chains to within 100 nanoseconds has only been partially attacked. Part of the problem, as you have seen, is the 5 microsecond ambiguity. That has a historical reason. Many of the loop antennas which were used in the past had the arrow pointed in the wrong direction. If you have stations which have the 5 microsecond offset, my recommendation would be to simply turn the loop around and the receiver will lock on. Except, it not quite as simple as that because the offset also affects the envelope synchronization. You have alluded to that problem. Let me say that all these things have to be precisely nailed down before you can make an adjustment. As funding becomes available, these questions will be resolved.